Journal of Physics: Conference Series

**PAPER** • **OPEN ACCESS**

# Orbit state deviation prediction model with second-order correction due to the $J_2$ term

To cite this article: Lei Wang *et al* 2018 *J. Phys.: Conf. Ser.* **1074** 012104





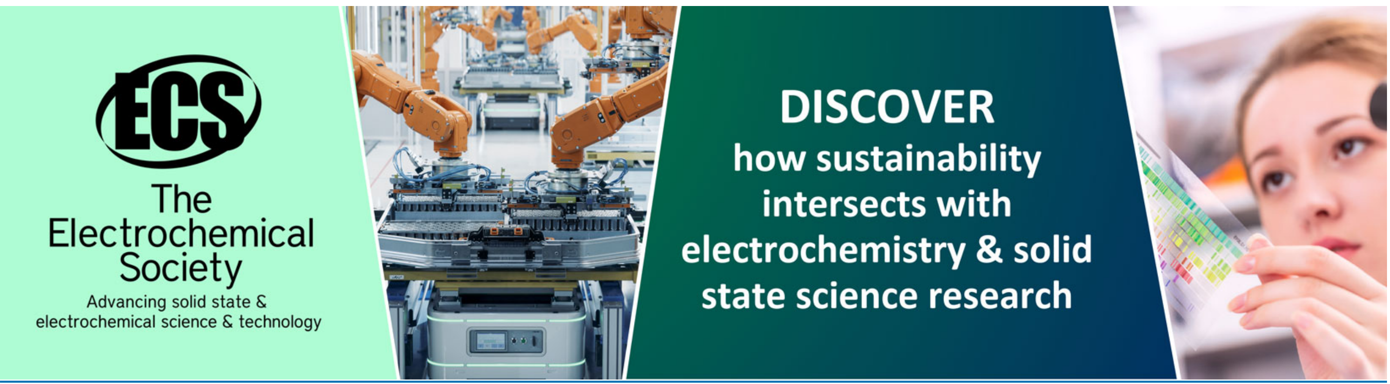

# Orbit state deviation prediction model with second-order correction due to the $J_2$ term

**Lei Wang[1], Wei Zheng and Xiang Zhou**

College of Aerospace Science and Engineering, National University of Defense Technology, No. 109, Deya Road, Changsha, China.

[1] E-mail : wanglei_nudt@163.com

**Abstract**. The analytic orbit state deviation prediction model derived based on the State Space Perturbation Method (SSPM) has proven effective and efficient to predict the impact error of ballistic missile caused by the $J_2$ term. However, the accuracy of this analytic model declines when the prediction point is located in the ascending portion of an orbit with large eccentricity. To deal with this problem, a second-order correction algorithm is proposed in this paper by deriving the partial derivatives of the analytic integral function with respect to the reference two-body orbit parameters. Three application scenarios are adopted to verify the accuracy of the proposed orbit state deviation prediction model, namely orbit injection point deviation prediction of carrier rocket, impact deviation prediction of ballistic missile and re-entry point deviation prediction of space shuttle. The accuracy of the proposed model is compared with the one without second-order correction as well as the Kozai's solution. Simulation results show that the proposed model has high precision in each case.

## 1. Introduction

The orbit prediction and correction is always the fundamental problem of celestial mechanics. For a spacecraft (e.g. satellite or rockets) moving under the effect of Earth's oblateness, namely the second zonal harmonic $J_2$ in the gravitational potential field, the orbit is no longer a standard ellipse. Analyzing the influence to orbit by geophysical perturbation factors essentially belongs to spacecraft orbit perturbation problem. Generally, methods utilized to deal with this problem can be classified into the special perturbation method and the general perturbation method [1]. The former uses direct numerical integration to get an exact solution, which mainly includes the Cowell's method and the Encke's method, while the latter normally obtains an approximate analytical solution through power series expansion, which mainly consists of the average methods with Brouwer-type or Kozai-type, the non-singular analytical method in terms of K-S elements and the linearization method.

The average methods have been greatly developed and widely used in the field of artificial satellites in recent decades since they were derived by Brouwer [2] and Kozai [3], and many improvements have been done after their pioneering work [4-8]. However, many of these theories which use mean elements are very difficult to implement for on-board real-time computation because of their complexity, and the mean elements should be calculated by some iterative algorithms from the initial osculating elements which also limits their computational efficiency.

Of all the perturbation methods, the linearization method does not provide an exact description of the motion but is an enormously valuable tool when used for short-term orbit prediction. Basically, the approach is to linearize the equations of motion by a series expansion about a nominal or reference orbit in which only first-order terms are retained. For the results to remain valid it is necessary to restrict the magnitude of the deviations from the nominal orbit. Ren [9] initially derived the analytical solution of the state transition matrix for the classical perturbed Keplerian motion with respect to the six-dimension state vector. Zheng [10] improved this method and named it State Space Perturbation Method (SSPM) in his PhD's thesis, and then used it to predict the trajectory of rocket in its coast phase. Wang [11] derived an analytic orbit state deviation prediction model with respect to the $J_2$ perturbation of the earth, and it has high accuracy for the applications of ballistic missile's impact point prediction. However, the accuracy of this analytic model declines when the prediction point is located in the ascending portion of an orbit with large eccentricity.

To deal with this problem, this paper proposes a second-order correction algorithm by deriving the partial derivatives of the analytic integral function with respect to the reference two-body orbit parameters. Simulation results show that the proposed model has high precision in different application scenarios.

## 2. Perturbed dynamics model of spacecraft

### 2.1. Perturbed differential equation

The perturbed differential equation of spacecraft's motion in the Local-Vertical-Local-Horizontal (LVLH) frame can be expressed as

$$\begin{cases} v_r' = v_f - \dfrac{\mu}{r v_f} + \dfrac{r}{v_f}\delta_r, & r' = \dfrac{r v_r}{v_f} \\ v_f' = -v_r + \dfrac{r}{v_f}\delta_f, & t' = \dfrac{r}{v_f} \\ v_z' = -\dfrac{z}{r}\dfrac{\mu}{v_f} + \dfrac{r}{v_f}\delta_z, & z' = \dfrac{r v_z}{v_f} \end{cases} \tag{1}$$

and, figure 1 shows the perturbed motion of spacecraft in the LVLH frame. The superscript of ' in Eq.(1) denotes the differential operator with respect to the true anomaly $f$ , and $v_r$ , $v_f$ and $v_z$ are the components of the velocity vector in the LVLH frame. $r$ and $z$ are the components of position vector in the LVLH frame. $t$ denotes the flight time of spacecraft from the initial point. $\delta_r$, $\delta_f$ and $\delta_z$ are the components of the perturbing force vector in the LVLH frame, and $\mu$ is the gravitational constant of the earth.

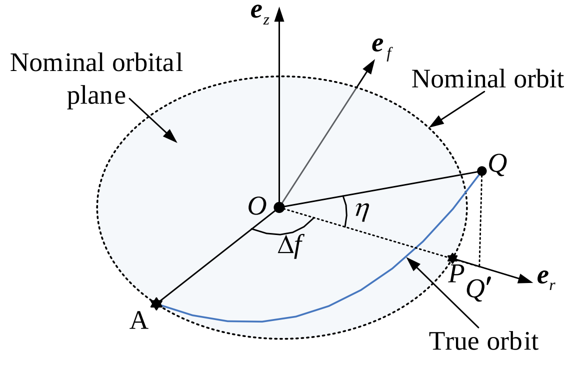


**Figure 1.** The perturbed motion of a body in the LVLH frame.

Let $\boldsymbol{X}_{ref}$ and $\boldsymbol{X}$ respectively represent the nominal state vector and true state vector of spacecraft, or,

$$\begin{aligned} \boldsymbol{X}_{ref} &= [v_{r,ref}, r_{ref}, v_{f,ref}, t_{ref}, v_{z,ref}, z_{ref}] \\ \boldsymbol{X} &= [v_r, r, v_f, t, v_z, z] \end{aligned} \tag{2}$$

then the differential equation of for nominal motion and true motion in vector style can be written as

$$\dot{\boldsymbol{X}}_{ref} = \boldsymbol{F}(\boldsymbol{X}_{ref}, f) \tag{3}$$

$$\dot{\boldsymbol{X}} = \boldsymbol{F}(\boldsymbol{X}, f) + \boldsymbol{U}(\boldsymbol{X}, f) \tag{4}$$

It is noticed that the perturbation term $\boldsymbol{U}(\boldsymbol{X}, f)$ is small. Let expand Eq.(4) at Eq.(3) by Taylor series and retain the first-order term, then one gets

$$\Delta\dot{\boldsymbol{X}} = \left.\frac{\partial \boldsymbol{F}}{\partial \boldsymbol{X}}\right|_{\boldsymbol{X}_{ref}} \Delta\boldsymbol{X} + \boldsymbol{U}(\boldsymbol{X}, f) \tag{5}$$

And we have [10]

$$\left.\frac{\partial \boldsymbol{F}}{\partial \boldsymbol{X}}\right|_{\boldsymbol{X}_{ref}} = \begin{bmatrix} 0 & \dfrac{\mu}{rh} & 1+\dfrac{r}{p} & 0 & 0 & 0 \\ \dfrac{r^2}{h} & \dfrac{rv_r}{h} & \dfrac{-r^3 v_r}{h^2} & 0 & 0 & 0 \\ -1 & 0 & 0 & 0 & 0 & 0 \\ 0 & \dfrac{r}{h} & -\dfrac{r^3}{h^2} & 0 & 0 & 0 \\ 0 & 0 & 0 & 0 & 0 & -\dfrac{\mu}{rh} \\ 0 & 0 & 0 & 0 & \dfrac{r^2}{h} & 0 \end{bmatrix}, \quad \boldsymbol{U}(\boldsymbol{X}, f) = \begin{bmatrix} \dfrac{r^2}{h}\delta_r \\ 0 \\ \dfrac{r^2}{h}\delta_f \\ 0 \\ \dfrac{r^2}{h}\delta_z \\ 0 \end{bmatrix} \tag{6}$$

where $\Delta\boldsymbol{X}$ is called the state deviation vector, i.e. $\Delta\boldsymbol{X} = \boldsymbol{X} - \boldsymbol{X}_{ref}$ . $h$ is the magnitude of angular momentum vector and $p$ is the semi-latus rectum of the nominal orbit.

### 2.2. J$_2$ term gravity expression in the LVLH frame

The gravity vector of J$_2$ term in the LVLH frame can be expressed as [11]

$$\begin{cases} \delta_r = \dfrac{\partial U_2}{\partial r} = -\dfrac{3K}{r_{ref}^4}(q_0 + q_1\cos 2f + q_2 \sin 2f) = -\dfrac{3K}{r_{ref}^4}T_1(f) \\ \delta_f = \dfrac{1}{r}\dfrac{\partial U_2}{\partial f} = \dfrac{2K}{r_{ref}^4}(-q_3\sin 2f + q_4\cos 2f) = \dfrac{2K}{r_{ref}^4}T_2(f) \\ \delta_z = \dfrac{1}{r}\dfrac{\partial U_2}{\partial z} = \dfrac{K}{r_{ref}^4}(q_1\cos f + q_2\sin f) = \dfrac{K}{r_{ref}^4}T_3(f) \end{cases} \tag{7}$$

Where $U_2$ presents the gravitational potential of the J$_2$ term, $K = 3J_2\mu a_e^2/4$ . $q_k$ $(k = 0,1,2,3,4)$ are constant coefficients.

### 2.3. Analytic integral function

The six-dimensional state transition matrix $\boldsymbol{\Phi}(f_1, f_0)$ for the state deviation differential equation (5) has be derived by a crafty transformation in [11]. According to the linear system theory, for systems of being subjected to continuous changed disturbance, the state vector at $f_1$ can be calculated by the initial conditions of $\Delta\boldsymbol{X}(f_0)$, as following

$$y_k(f_1)=\int_{f_0}^{f_1}\frac{1}{h}r_{ref}^2(\xi)\left[\lambda_{k,1}(f_1,\xi)\delta_r(\xi)+\lambda_{k,3}(f_1,\xi)\delta_f(\xi)+\lambda_{k,5}(f_1,\xi)\delta_z(\xi)\right]\mathrm{d}\xi \tag{8}$$

Where $y_k(f_1)$ denotes the component of $\Delta\boldsymbol{X}(f_1)$ and $\lambda_{k,j}(f_1,\xi)$ denote the element of $\boldsymbol{\Phi}(f_1, f_0)$ located at the $k^{\text{th}}$ row and $j^{\text{th}}$ column.

## 3. Second-order correction algorithm

From Eq.(8), we can know that the value of the integrand function in each integral step is determined by the reference orbit parameters. However, the true orbit parameters are changing all the time due to the $J_2$ perturbation. Let's rewrite the expression (8) as,

$$y_k=\int_{f_0}^{f_1}\left[H_{1,k}(\boldsymbol{X}_{ref},\xi)\cdot T_1(\xi)+H_{2,k}(\boldsymbol{X}_{ref},\xi)\cdot T_2(\xi)+H_{3,k}(\boldsymbol{X}_{ref},\xi)\cdot T_3(\xi)\right]d\xi \tag{9}$$

where $H_{n,k}(\boldsymbol{X}_{ref},\xi)$ represents the integrand function which is related to the reference orbit parameters. If the state deviation vector $y_k(\xi)$ at every locations on the reference orbit are given, we can obtain the second-order correction values for each component of $y_k(\xi)$

$$\begin{aligned}\Delta y_k=\int_{f_0}^{f_1}\Bigg[&\left(\frac{\partial H_{1,k}}{\partial v_{r,ref}}y_1(\xi)+\frac{\partial H_{1,k}}{\partial r_{ref}}y_2(\xi)+\frac{\partial H_{1,k}}{\partial v_{f,ref}}y_3(\xi)\right)\cdot T_1(\xi)\\&+\left(\frac{\partial H_{2,k}}{\partial v_{r,ref}}y_1(\xi)+\frac{\partial H_{2,k}}{\partial r_{ref}}y_2(\xi)+\frac{\partial H_{2,k}}{\partial v_{f,ref}}y_3(\xi)\right)\cdot T_2(\xi)\\&+\left(\frac{\partial H_{3,k}}{\partial v_{r,ref}}y_1(\xi)+\frac{\partial H_{3,k}}{\partial r_{ref}}y_2(\xi)+\frac{\partial H_{3,k}}{\partial v_{f,ref}}y_3(\xi)\right)\cdot T_3(\xi)\Bigg]d\xi\end{aligned} \tag{10}$$

The partial derivatives with respect to the position components are listed below,

$$\frac{\partial H_{1,2}}{\partial v_{r,ref}}=-\frac{6Kr_1^3}{h^3}\frac{1}{r_\xi^2}\sin^2(f_1-\xi) \tag{11}$$

$$\frac{\partial H_{1,2}}{\partial r_{ref}}=\frac{6Kr_1^3}{h^2}\frac{1}{r_\xi^4}\sin(f_1-\xi)\cos(f_1-\xi)-\frac{6Kr_1^3e}{h^2p}\frac{1}{r_\xi^3}\sin(\xi)\sin^2(f_1-\xi) \tag{12}$$

$$\frac{\partial H_{1,2}}{\partial v_{f,ref}}=\frac{12Kr_1^3}{h^3}\frac{1}{r_\xi^2}\sin(f_1-\xi)\cos(f_1-\xi)-\frac{6Kr_1^3e}{h^3p}\frac{1}{r_\xi}\sin(\xi)\sin^2(f_1-\xi)-\frac{6Kr_1^2}{h^3}\frac{1}{r_\xi}\sin(f_1-\xi) \tag{13}$$

$$\begin{aligned}\frac{\partial H_{2,2}}{\partial v_{r,ref}}=&\left(\frac{8Kr_1^3}{h^3p}-\frac{2Kr_1^2}{h^3}\right)\frac{1}{r_\xi}\sin(f_1-\xi)-\frac{8Kr_1^3}{h^3p}\frac{1}{r_\xi}\sin(f_1-\xi)\cos(f_1-\xi)\\&+\frac{8Kr_1^3}{h^3p}\frac{1}{r_\xi}\sin(f_1-\xi)-\frac{4Kr_1^3e}{h^3p}\frac{1}{r_\xi}\sin(\xi)\sin^2(f_1-\xi)\end{aligned} \tag{14}$$

$$\begin{aligned}\frac{\partial H_{2,2}}{\partial r_{ref}} &= \frac{4Kr_1^2}{h^2 p}\frac{1}{r_\xi^2}\cos(f_1-\xi) - \frac{4Kr_1^2}{h^2 p}\frac{1}{r_\xi^2} + \frac{8Kr_1^3}{h^2 p}\frac{1}{r_\xi^3}\cos(f_1-\xi)\cos(f_1-\xi) - \frac{8Kr_1^3}{h^2 p}\frac{1}{r_\xi^3}\cos(f_1-\xi)\\ &+\frac{4Kr_1^3 e}{h^2 p}\frac{1}{r_\xi^3}\sin(\xi)\cos(f_1-\xi)\sin(f_1-\xi) - \frac{8Kr_1^3 e}{h^2 p^2}\frac{1}{r_\xi^2}\sin(\xi)\cos(f_1-\xi)\sin(f_1-\xi)\\ &+\frac{8Kr_1^3 e}{h^2 p^2}\frac{1}{r_\xi^2}\sin(\xi)\sin(f_1-\xi) - \frac{4Kr_1^3 e^2}{h^2 p^2}\frac{1}{r_\xi^2}\sin^2(\xi)\sin^2(f_1-\xi)\end{aligned} \tag{15}$$

$$\begin{aligned}\frac{\partial H_{2,2}}{\partial v_{f,ref}} &= \frac{16Kr_1^3}{h^3 p}\frac{1}{r_\xi}\cos(f_1-\xi)\cos(f_1-\xi) - \frac{16Kr_1^3}{h^3 p}\frac{1}{r_\xi}\cos(f_1-\xi)\\ &+\frac{8Kr_1^3 e}{h^3 p}\frac{1}{r_\xi}\sin(\xi)\cos(f_1-\xi)\sin(f_1-\xi) - \frac{8Kr_1^3 e}{h^3 p^2}\sin(\xi)\cos(f_1-\xi)\sin(f_1-\xi)\\ &+\left(\frac{8Kr_1^3 e}{h^3 p^2} - \frac{2Kr_1^2 e}{h^3 p}\right)\sin(\xi)\sin(f_1-\xi) - \frac{4Kr_1^3 e^2}{h^3 p^2}\sin^2(\xi)\sin^2(f_1-\xi)\end{aligned} \tag{16}$$

$$\frac{\partial H_{3,2}}{\partial v_{r,ref}} = \frac{\partial H_{3,2}}{\partial r_{ref}} = \frac{\partial H_{3,2}}{\partial v_{f,ref}} = 0 \tag{17}$$

$$\frac{\partial H_{3,6}}{\partial v_{r,ref}} = \frac{2Kr_1^2}{h^3}\frac{1}{r_\xi}\sin(f_1-\xi) \tag{18}$$

$$\frac{\partial H_{3,6}}{\partial r_{ref}} = \left(\frac{2Kr_1^2}{h^2 p} - \frac{4Kr_1}{h^2}\right)\frac{1}{r_\xi^2} - \frac{2Kr_1^2}{h^2 p}\frac{1}{r_\xi^2}\cos(f_1-\xi) \tag{19}$$

$$\frac{\partial H_{3,6}}{\partial v_{f,ref}} = \left(\frac{2Kr_1^2}{h^3 p} - \frac{2Kr_1}{h^3}\right) - \frac{2Kr_1^2}{h^3 p}\cos(f_1-\xi) - \frac{2Kr_1^2}{h^3}\frac{1}{r_\xi}\cos(f_1-\xi) \tag{20}$$

$$\frac{\partial H_{1,6}}{\partial v_{r,ref}} = \frac{\partial H_{1,6}}{\partial r_{ref}} = \frac{\partial H_{1,6}}{\partial v_{f,ref}} = \frac{\partial H_{2,6}}{\partial v_{r,ref}} = \frac{\partial H_{2,6}}{\partial r_{ref}} = \frac{\partial H_{2,6}}{\partial v_{f,ref}} = 0 \tag{21}$$

It is noticed that the $y_k(\xi)$ should be known when we want to calculate the second-order correction values according to Eq.(10). Here, we introduce a possible strategy to deal with this problem. Firstly, selecting a set of reference points between the initial point and prediction point, and usually five points are enough if the true anomaly interval is less than 180 degrees. Secondly, calculating the state deviations on these selected points based on Eq.(8). Finally, fitting every components of the state deviation vector based on the following function

$$y_k^i = a_k^0 + a_k^1 \sin f + a_k^2 \cos f + a_k^3 \cos^2 f + a_k^4 \cos f \sin f \tag{22}$$

## 4. Simulation

Numerical simulations are conducted in this section to verify the effectiveness of the proposed model. The state deviations caused by the Earth's oblateness are calculated by numerical integration, the orbit state deviation prediction mode without correction, the proposed method in this paper. The results calculated by numerical integration are regarded as the standard for accuracy estimate, and the residual errors of position are focused to reveal the presented method's accuracy in different initial conditions.

Besides, the first-order analytic solution based on Lagrange's planetary equation with the same perturbing acceleration investigated by Kozai has also been used to compare with the presented method, and the first-order and second-order secular terms, first-order long period term and short period term are considered in this solution, and the second-order effects of semi-major axis is also calculated in order to guarantee the computation precision of mean anomaly.

Three simulation cases are conducted to verify the accuracy of the proposed orbit state deviation prediction model, namely orbit injection point deviation prediction of carrier rocket, impact deviation prediction of ballistic missile and re-entry point deviation prediction of space shuttle. The initial conditions for these three cases are listed in table 1.

**Table 1.** Initial Conditions.

| Parameters | | Symbols | Values | | |
|---|---|---|---|---|---|
| | | | Case A | Case B | Case C |
| Semi-major axis | (km) | $a$ | 6378 | 6178 | 6978 |
| Eccentricity | | $e$ | 0.5 | 0.43 | 0.3 |
| Inclination | deg | $i$ | 0-180 | 0-180 | 0-180 |
| RAAN | deg | $\Omega$ | 0 | 0 | 0 |
| Argument of perigee | deg | $\omega$ | 270 | 270 | 270 |
| Initial true anomaly | deg | $f_0$ | 60 | 120 | 180 |
| Terminal true anomaly | deg | $f_1$ | 180 | 240 | 300 |

Figure 2, 4 and 6 show the position deviations caused by the J2 term for these three cases, and all these values are calculated by numerical integral. It is noticed that the maximum position deviation for these three cases exceed 65 km, 12 km and 8 km, respectively. Moreover, the maximum value appears at inclination equal 0, 90 and 180 degrees.

Figure 3, 5 and 7 illustrate the computation residuals of the position deviation for these three cases. It is clear that the presented model has high precision in each case, while the accuracy of the analytical solution without second-order correction for case A declines dramatically.

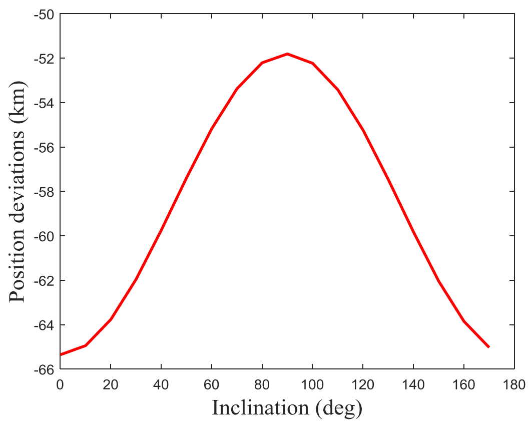


**Figure 2.** Position deviation caused by J2 for case A.

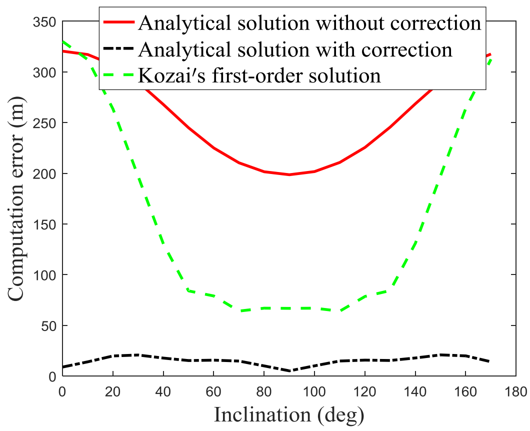


**Figure 3.** Computation residuals for different solutions for case A.

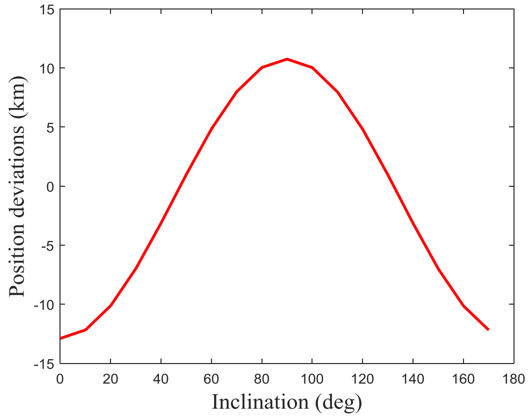


**Figure 4.** Position deviation caused by J2 for case B.

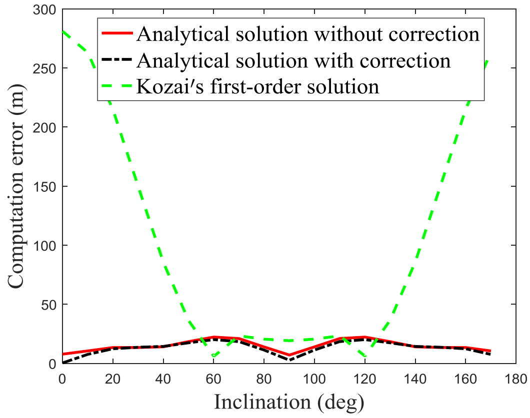


**Figure 5.** Computation residuals for different solutions for case B.

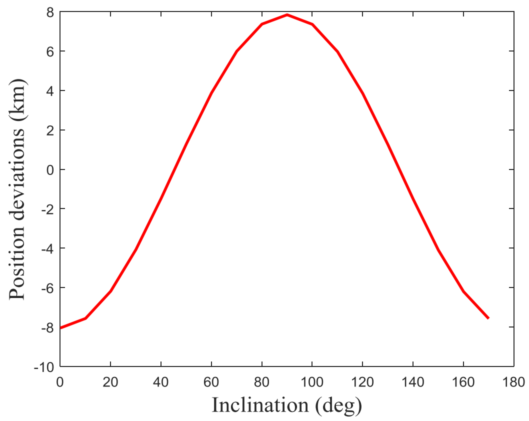


**Figure 6.** Position deviation caused by J2 for case C.

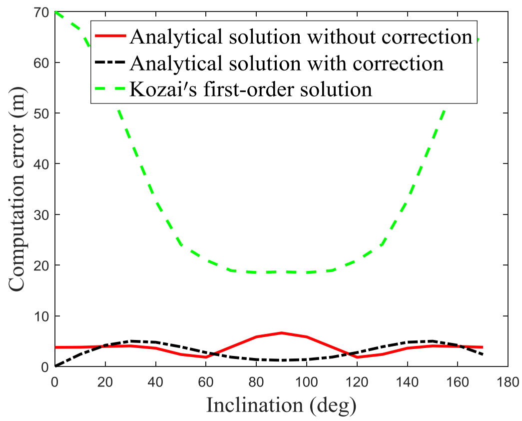


**Figure 7.** Computation residuals for different solutions for case C.

## 5. Conclusions

In order to overcoming the descent of precision for the analytic orbit state deviation prediction model when the prediction point is located in the ascending portion of an orbit with large eccentricity, a second-order correction algorithm is proposed in this paper by deriving the partial derivatives of the analytic integral function with respect to the reference two-body orbit parameters. Three application scenarios are adopted to verify the accuracy of the proposed orbit state deviation prediction model, namely orbit injection point deviation prediction of carrier rocket, impact deviation prediction of ballistic missile and re-entry point deviation prediction of space shuttle. The accuracy of the proposed model is compared with the one without second-order correction as well as the Kozai's solution. Simulation results show that the proposed model has high precision in each application cases.

## References

[1] Battin R H 1999 *An introduction to the mathematics and methods of astrodynamics* (Revised Edition) AIAA Education Series Reston VA p 434-448
[2] Brouwer D 1959 Solution of the Problem of Artificial Satellite Theory without Drag. *Astronomical Journal* **64** 378-397
[3] Kozai Y 1959 The Motion of a Close Earth Satellite *Astron. J.* **64** 367-377
[4] Kozai Y 1962 Second-Order Solution of Artificial Satellite Theory without Air Drag *Astronomical Journal* **67** 446-461

[5] Deprit A 1981 The elimination of the parallax in satellite theory *Celestial Mechanics* **24** 111-153
[6] Gurfil P and Lara M 2014 Satellite onboard orbit propagation using Deprit's radial intermediary *Celestial Mechanics & Dynamical Astronomy* **120** 217-232
[7] Hautesserres D and Lara M 2017 Intermediary LEO propagation including higher order zonal harmonics *Celestial Mechanics & Dynamical Astronomy* **127** 505-526
[8] Sharma R K and Raj M X J 2010 Analytical approach using KS elements to high eccentricity orbit predictions including drag *Acta Astronaut* **66** 864-870
[9] Ren X 1984 The influence of gravity anomaly on motion of the ballistic missile: influence on unpowered-flight phase *National University of Defense Technology* **7** 63-82
[10] Zheng W and Tang G 2009 *Flight dynamics of ballistic missile in gravity anomaly field*. Beijing: National Defense Industry Press p 46-72
[11] Wang L and Zheng W 2018 Approximate analytic solution of motion for spacecraft around an oblate planet *Proc. IMechE. Part G: Journal of Aerospace Engineering* doi: 10.1177/0954410017752526